$$\left[r_{SR}+\frac{V_{RS}}{c}\left|\boldsymbol{\mathcal{R}}_{TS}(t')\right|\right]^2=r_{SR}^2+2r_{SR}\frac{V_{RS}}{c}\left|\boldsymbol{\mathcal{R}}_{TS}(t')\right|+\left(\frac{V_{RS}}{c}\right)^2\left|\boldsymbol{\mathcal{R}}_{TS}(t')\right|^2>0\,, \tag{10C-1}$$

or

$$r_{SR}^2+\left(\frac{V_{RS}}{c}\right)^2\left|\boldsymbol{\mathcal{R}}_{TS}(t')\right|^2>-2r_{SR}\frac{V_{RS}}{c}\left|\boldsymbol{\mathcal{R}}_{TS}(t')\right|, \tag{10C-2}$$

where the left-hand side of (10C-2) is equal to the sum of the first and third terms in (10.7-40).

Next we shall show that the right-hand side of (10C-2) is equal to the most negative value of the second term in (10.7-40). The second term in (10.7-40) can be rewritten as follows:

$$\begin{aligned}2r_{SR}\frac{\hat{r}_{SR}\bullet\mathbf{V}_{RS}}{c}\left|\boldsymbol{\mathcal{R}}_{TS}(t')\right|&=2r_{SR}\frac{\left|\hat{r}_{SR}\right|\left|\mathbf{V}_{RS}\right|\cos\delta}{c}\left|\boldsymbol{\mathcal{R}}_{TS}(t')\right|\\&=2r_{SR}\frac{V_{RS}\cos\delta}{c}\left|\boldsymbol{\mathcal{R}}_{TS}(t')\right|,\end{aligned} \tag{10C-3}$$

where δ is the angle between the unit vector $\hat{r}_{SR}$ and the relative velocity vector $\mathbf{V}_{RS}$. If $\delta=\pi$, then

$$2r_{SR}\frac{\hat{r}_{SR}\bullet\mathbf{V}_{RS}}{c}\left|\boldsymbol{\mathcal{R}}_{TS}(t')\right|=-2r_{SR}\frac{V_{RS}}{c}\left|\boldsymbol{\mathcal{R}}_{TS}(t')\right|, \tag{10C-4}$$

where the right-hand side of (10C-4) is equal to the right-hand side of (10C-2). Therefore, since (10C-2) shows that the sum of the first and third terms in (10.7-40) is always greater than the most negative value of the second term in (10.7-40), $\mathcal{C}>0$.

Chapter 11

Real Bandpass Signals and Complex Envelopes

11.1 Definitions and Basic Relationships

Real world transmitted electrical signals used in *active* sonar and radar systems, and communication systems, belong to a class of signals known as *amplitude-and-angle-modulated carriers*. Amplitude-and-angle-modulated carriers are *real bandpass signals*. In this section we shall discuss how to represent a real bandpass signal in terms of its *complex envelope*. As will be shown later, a complex envelope is, in general, a *complex signal* with a *lowpass (baseband)* frequency spectrum. One of the main advantages of expressing real bandpass signals in terms of their complex envelopes is that it provides for a simple representation of amplitude-and-angle-modulated carriers, which is very useful for doing analysis. For example, in Chapter 12, we will derive the *auto-ambiguity function*, which is used as a measure of the range and Doppler resolving capabilities of different transmitted electrical signals (amplitude-and-angle-modulated carriers) used in active sonar and radar systems. The complex envelope of a signal is required in order to compute its ambiguity function.

Let $x(t)$ be a *real bandpass signal* with magnitude spectrum $|X(f)|$ centered at $f = \pm f_c$ hertz (see Fig. 11.1-1), where

$$X(f) = F\{x(t)\} = \int_{-\infty}^{\infty} x(t)\exp(-j2\pi ft)\,dt \tag{11.1-1}$$

and f_c is referred to as either the *center frequency* or *carrier frequency*. If $x(t)$ has units of volts (or amperes), then $X(f)$ will have units of volts (or amperes) per hertz. As shown in Fig. 11.1-1, the bandwidth of $x(t)$ is $2W$ hertz. Bandwidth is always measured along the *positive* frequency axis. There are two kinds of bandpass signals, *narrowband* and *broadband* (a.k.a. wideband). A narrowband bandpass signal satisfies the inequality $2W/f_c << 1$, or equivalently, $2W/f_c \le 0.1$. Therefore, a broadband (wideband) bandpass signal satisfies the inequality $2W/f_c > 0.1$.

The *complex envelope* of $x(t)$, denoted by $\tilde{x}(t)$, is defined as follows:

$$\boxed{\tilde{x}(t) \triangleq x_p(t)\exp(-j2\pi f_c t)} \tag{11.1-2}$$

where

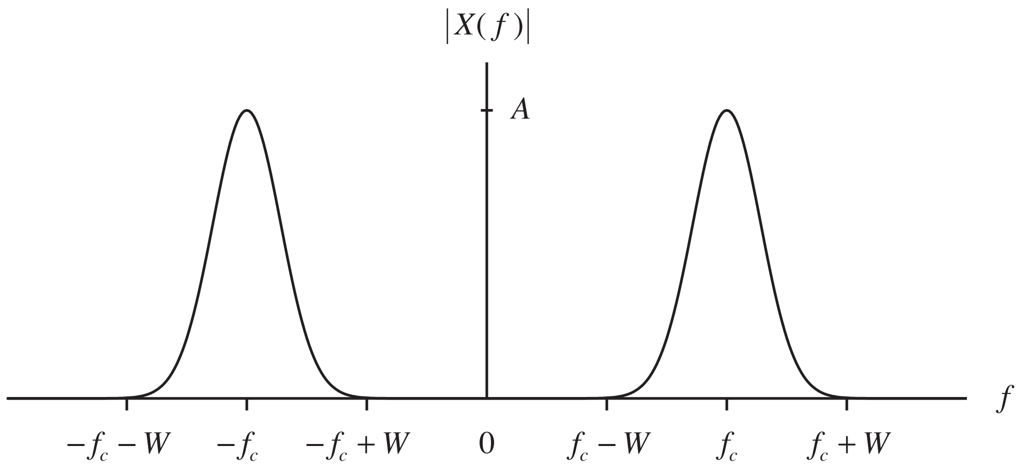

Figure 11.1-1 Magnitude spectrum of a real bandpass signal $x(t)$ with bandwidth $2W$ hertz.

$$\boxed{x_p(t) = x(t) + j\hat{x}(t)} \tag{11.1-3}$$

is the *pre-envelope* (a.k.a. the *analytic signal*) of $x(t)$, and $\hat{x}(t)$ is the *Hilbert transform* of $x(t)$. Solving for $x_p(t)$ using (11.1-2) yields

$$x_p(t) = \tilde{x}(t)\exp(+j2\pi f_c t), \tag{11.1-4}$$

and from (11.1-3),

$$x(t) = \text{Re}\left\{x_p(t)\right\}, \tag{11.1-5}$$

where Re means "take the real part." Substituting (11.1-4) into (11.1-5) yields

$$\boxed{x(t) = \text{Re}\left\{\tilde{x}(t)\exp(+j2\pi f_c t)\right\}} \tag{11.1-6}$$

Therefore, given a complex envelope $\tilde{x}(t)$, the corresponding real bandpass signal $x(t)$ can be obtained from (11.1-6).

The *envelope* of $x(t)$, denoted by $\mathcal{E}(t)$, is defined as follows:

$$\boxed{\mathcal{E}(t) \triangleq \text{Abs}\left\{\left|\tilde{x}(t)\right|\right\} \geq 0} \tag{11.1-7}$$

where Abs means "take the absolute value." At first glance it would seem that taking the absolute value of the magnitude of a complex signal is redundant.

However, since the magnitude of the complex envelope is, in general, a real-valued function of time that can take on both positive and negative values, in order to ensure that the envelope $\mathcal{E}(t)$ is nonnegative (analogous to the output from an envelope detector), we must also take the absolute value.

As can be seen from (11.1-2) and (11.1-3), in order to compute the complex envelope of $x(t)$, we first need to compute the Hilbert transform of $x(t)$. One way to compute the Hilbert transform is to perform the following inverse Fourier transform:

$$\boxed{\hat{x}(t) = F^{-1}\{-j\,\mathrm{sgn}(f)X(f)\}} \tag{11.1-8}$$

where

$$\mathrm{sgn}(f) = \begin{cases} 1, & f > 0 \\ 0, & f = 0 \\ -1, & f < 0 \end{cases} \tag{11.1-9}$$

is the *signum* or *sign function*, and $X(f)$ is the Fourier transform of $x(t)$ given by (11.1-1). Therefore, from (11.1-8), the Fourier transform of the Hilbert transform of $x(t)$ is given by

$$\boxed{\hat{X}(f) = F\{\hat{x}(t)\} = -j\,\mathrm{sgn}(f)X(f)} \tag{11.1-10}$$

The Hilbert transform is basically a $90°$ phase-shifter. This can easily be shown by using (11.1-8) and (11.1-9). For positive frequencies ($f > 0$),

$$\hat{x}(t) = F^{-1}\{-jX(f)\} = F^{-1}\{\exp(-j\pi/2)X(f)\}, \qquad f > 0, \tag{11.1-11}$$

which corresponds to a $-90°$ phase shift, and for negative frequencies ($f < 0$),

$$\hat{x}(t) = F^{-1}\{+jX(f)\} = F^{-1}\{\exp(+j\pi/2)X(f)\}, \qquad f < 0, \tag{11.1-12}$$

which corresponds to a $+90°$ phase shift. Therefore, the magnitude spectrum of a bandpass signal is not altered by a Hilbert transform – only the phase spectrum is. If we denote the Hilbert transform by $H\{\bullet\}$, then it can be shown that

$$H\{\cos(2\pi f_c t + \theta_0)\} = \sin(2\pi f_c t + \theta_0) = \cos\left(2\pi f_c t + \theta_0 - \frac{\pi}{2}\right) \tag{11.1-13}$$

and

$$H\{\sin(2\pi f_c t + \theta_0)\} = -\cos(2\pi f_c t + \theta_0) = \sin\left(2\pi f_c t + \theta_0 - \frac{\pi}{2}\right) \tag{11.1-14}$$

where θ_0 is a constant phase angle in radians. The right-hand sides of (11.1-13) and (11.1-14) are simply trigonometric identities.

Next we shall show that the complex envelope of a real bandpass signal has a lowpass (baseband) frequency spectrum. Taking the Fourier transform of (11.1-2) and (11.1-3) yields

$$\boxed{\tilde{X}(f) = X_p(f + f_c)} \tag{11.1-15}$$

and

$$X_p(f) = X(f) + j\hat{X}(f)\,, \tag{11.1-16}$$

respectively, where

$$\tilde{X}(f) = F\{\tilde{x}(t)\} \tag{11.1-17}$$

and

$$X_p(f) = F\{x_p(t)\}\,. \tag{11.1-18}$$

Substituting (11.1-10) into (11.1-16) yields

$$X_p(f) = \left[1 + \operatorname{sgn}(f)\right]X(f)\,, \tag{11.1-19}$$

and with the use of (11.1-9),

$$\boxed{X_p(f) = \begin{cases} 2X(f), & f > 0 \\ 0, & f \le 0 \end{cases}} \tag{11.1-20}$$

The frequency spectrum of the pre-envelope given by (11.1-20) is known as a *one-sided spectrum* because it only contains positive frequency components (see Fig. 11.1-2). Note that

$$\begin{aligned} X_p(0) &= \left[1 + \operatorname{sgn}(0)\right]X(0) \\ &= X(0) \\ &= 0 \end{aligned} \tag{11.1-21}$$

because $x(t)$ is a bandpass signal (see Fig. 11.1-1).

By referring to (11.1-15), it can be seen that the frequency spectrum of the complex envelope can be obtained by shifting the frequency spectrum of the pre-envelope to the left by an amount equal to the carrier frequency f_c, as shown in Fig. 11.1-3, thus creating a lowpass signal with bandwidth W hertz. This is another reason for representing a real bandpass signal in terms of its complex envelope because $\tilde{x}(t)$ can be sampled at the lower rate $f_S \ge 2W$ samples per second versus the higher rate $f_S \ge 2(f_c + W)$ samples per second for $x(t)$.

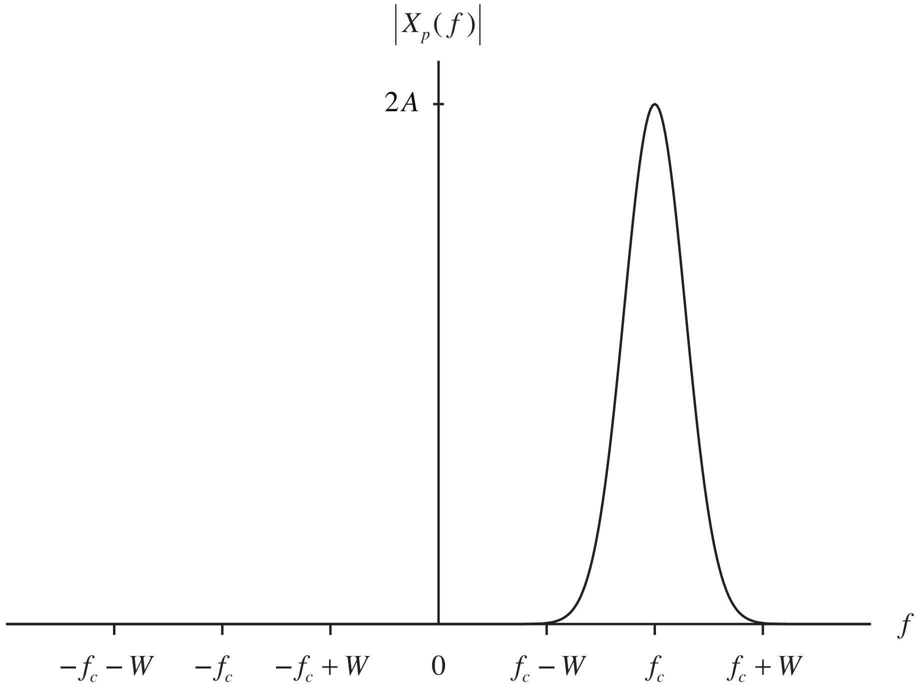

Figure 11.1-2 Magnitude spectrum of the pre-envelope $x_p(t)$ with bandwidth $2W$ hertz.

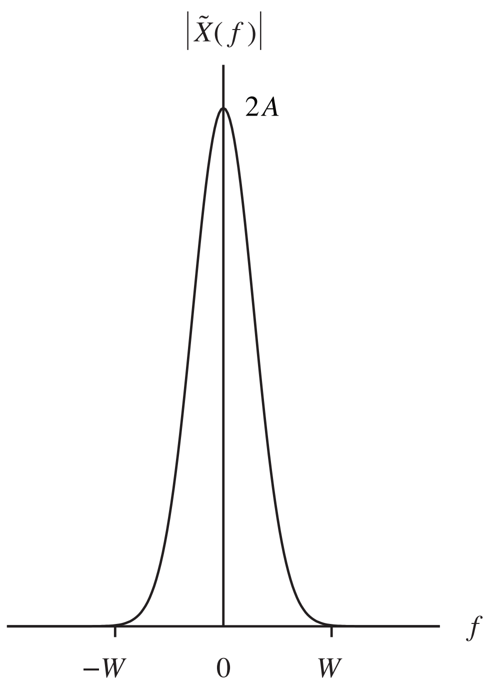

Figure 11.1-3 Magnitude spectrum of the lowpass complex envelope $\tilde{x}(t)$ with bandwidth W hertz.

We shall end our discussion in this section by deriving the relationship between the complex frequency spectrum $X(f)$ of the real bandpass signal $x(t)$ and the complex frequency spectrum $\tilde{X}(f)$ of its complex envelope $\tilde{x}(t)$. If Z is complex, then

$$\text{Re}\{Z\} = (Z + Z^*)/2 \,. \tag{11.1-22}$$

With the use of (11.1-22), (11.1-6) can be rewritten as

$$x(t) = \frac{1}{2}\left[\tilde{x}(t)\exp(+j2\pi f_c t) + \tilde{x}^*(t)\exp(-j2\pi f_c t)\right]. \tag{11.1-23}$$

Taking the Fourier transform of (11.1-23) yields

$$\boxed{X(f) = \frac{1}{2}\left[\tilde{X}(f - f_c) + \tilde{X}^*\left(-[f + f_c]\right)\right]} \tag{11.1-24}$$

where

$$F\left\{\tilde{x}(t)\exp(+j2\pi f_c t)\right\} = \tilde{X}(f - f_c)\,, \tag{11.1-25}$$

$$F\left\{\tilde{x}^*(t)\right\} = \tilde{X}^*(-f)\,, \tag{11.1-26}$$

and

$$F\left\{\tilde{x}^*(t)\exp(-j2\pi f_c t)\right\} = \tilde{X}^*\left(-[f + f_c]\right). \tag{11.1-27}$$

11.1.1 Signal Energy and Time-Average Power

In this subsection we shall relate the energy of a real bandpass signal (an amplitude-and-angle-modulated carrier) $x(t)$ to the energy of its complex envelope $\tilde{x}(t)$. We shall then use this energy relationship to compute the time-average power of $x(t)$.

From signal theory, the *energy* E_x of the real signal $x(t)$ is, by definition,

$$\boxed{E_x \triangleq \int_{-\infty}^{\infty} x^2(t)\,dt} \tag{11.1-28}$$

For example, if $x(t)$ is the instantaneous voltage (in volts) across a linear, time-invariant, resistive load, then E_x given by (11.1-28) has units of *joules-ohms*. However, if $x(t)$ is the instantaneous current (in amperes) flowing through a linear, time-invariant, resistive load, then E_x has units of *joules per ohm*. These units can easily be verified as follows: the instantaneous power $p(t)$ in watts is given by $p(t) = v(t)i(t)$, where $v(t)$ is the instantaneous voltage in volts, and $i(t)$ is the instantaneous current in amperes. For a linear, time-invariant, resistive load, Ohm's law states that $v(t) = Ri(t)$, where R is the constant resistance in ohms. Therefore, $p(t) = v^2(t)/R$ or $p(t) = Ri^2(t)$. Since energy E in joules is equal to the integral of instantaneous power $p(t)$ in watts, that is, since $E = \int p(t)\,dt$, then $E = R^{-1}\int v^2(t)\,dt$ has units of joules and $ER = \int v^2(t)\,dt$ has units of joules-ohms. In addition, $E = R\int i^2(t)\,dt$ has units of joules and $E/R = \int i^2(t)\,dt$ has units of joules per ohm. Therefore, if (11.1-28) is used to compute signal energy, divide or multiply your answer by the constant resistance R of the load to get energy in joules. For sonar applications, the load could be, for example, an electroacoustic transducer.

Similarly, the *energy* $E_{\tilde{x}}$ of the complex envelope $\tilde{x}(t)$ is, by definition,

$$\boxed{E_{\tilde{x}} \triangleq \int_{-\infty}^{\infty} \left|\tilde{x}(t)\right|^2 dt} \tag{11.1-29}$$

If $\tilde{x}(t)$ is the complex envelope of the instantaneous voltage (in volts) across a linear, time-invariant, resistive load, then $E_{\tilde{x}}$ given by (11.1-29) has units of *joules-ohms*. However, if $\tilde{x}(t)$ is the complex envelope of the instantaneous current (in amperes) flowing through a linear, time-invariant, resistive load, then $E_{\tilde{x}}$ has units of *joules per ohm*. By referring to (11.1-2) and (11.1-3), it can be seen that

$$\left|\tilde{x}(t)\right|^2 = x^2(t) + \hat{x}^2(t)\,. \tag{11.1-30}$$

Substituting (11.1-30) into (11.1-29) yields

$$E_{\tilde{x}} = E_x + E_{\hat{x}}\,, \tag{11.1-31}$$

where

$$E_{\hat{x}} = \int_{-\infty}^{\infty} \hat{x}^2(t)\,dt \tag{11.1-32}$$

is the energy of the Hilbert transform of $x(t)$. With the use of *Parseval's Theorem*, (11.1-32) can be expressed as

$$E_{\hat{x}} = \int_{-\infty}^{\infty} \left|\hat{X}(f)\right|^2 df\,, \tag{11.1-33}$$

and by substituting (11.1-10) into (11.1-33), we obtain

$$E_{\hat{x}} = \int_{-\infty}^{\infty} |X(f)|^2 \, df = \int_{-\infty}^{\infty} x^2(t) \, dt \,, \tag{11.1-34}$$

or

$$\boxed{E_{\hat{x}} = E_x} \tag{11.1-35}$$

Therefore, the real bandpass signal $x(t)$ and its Hilbert transform $\hat{x}(t)$ have equal energy. This is not surprising because the magnitude spectrum of a bandpass signal is not altered by a Hilbert transform – only the phase spectrum is [see (11.1-11) and (11.1-12)]. Substituting (11.1-35) into (11.1-31) yields the following important relationship:

$$\boxed{E_x = E_{\tilde{x}}/2} \tag{11.1-36}$$

As we shall show in Section 11.2, it is much easier to compute the energy of an amplitude-and-angle-modulated carrier (a real bandpass signal) by first computing the energy of its complex envelope and then dividing that energy by a factor of two.

In real-world problems, $x(t)$ will have a finite duration. If $x(t)$ is defined in the closed time interval $[0, T]$, that is, for $0 \le t \le T$, where T is the *duration* or *pulse length* of $x(t)$ in seconds, then the energies given by (11.1-28) and (11.1-29) reduce as follows:

$$E_x = \int_0^T x^2(t) \, dt \tag{11.1-37}$$

and

$$E_{\tilde{x}} = \int_0^T |\tilde{x}(t)|^2 \, dt \,. \tag{11.1-38}$$

The *time-average power* $P_{\mathrm{avg},x}$ of $x(t)$ in the time interval $[0, T]$ is given by

$$\boxed{P_{\mathrm{avg},x} = \frac{E_x}{T} = \frac{1}{T} \int_0^T x^2(t) \, dt} \tag{11.1-39}$$

and the *time-average power* $P_{\mathrm{avg},\tilde{x}}$ of $\tilde{x}(t)$ in the time interval $[0, T]$ is given by

$$\boxed{P_{\mathrm{avg},\tilde{x}} = \frac{E_{\tilde{x}}}{T} = \frac{1}{T} \int_0^T |\tilde{x}(t)|^2 \, dt} \tag{11.1-40}$$

If the energies in (11.1-39) and (11.1-40) have units of joules-ohms or joules per ohm, then the time-average powers in (11.1-39) and (11.1-40) will have units of watts-ohms or watts per ohm, respectively. Finally, note that

$$\boxed{P_{\text{avg},x} = \frac{1}{2} P_{\text{avg},\tilde{x}} = \frac{1}{2}\frac{E_{\tilde{x}}}{T} = \frac{E_x}{T}} \tag{11.1-41}$$

Knowing the time-average power of a transmitted electrical signal is important because electroacoustic transducers have limits on the maximum time-average power that they can handle before being damaged, and it is one of the parameters that determines the signal-to-noise ratio at a receiver.

11.1.2 The Power Spectrum

In this subsection we shall relate the power spectrum of a real bandpass signal (an amplitude-and-angle-modulated carrier) $x(t)$ to the power spectrum of its complex envelope $\tilde{x}(t)$. We shall then use the power spectrums of $x(t)$ and $\tilde{x}(t)$ to compute the time-average powers of $x(t)$ and $\tilde{x}(t)$.

The definition of the power spectrum $S_x(f)$ of a finite duration, deterministic signal $x(t)$ is given by

$$\boxed{S_x(f) \triangleq \frac{1}{T}\left|X(f)\right|^2} \tag{11.1-42}$$

where T is the duration or pulse length of $x(t)$ in seconds. From (11.1-42) it can be seen that the power spectrum $S_x(f)$ is *real* and *nonnegative*, that is, $S_x(f) \geq 0$. If $x(t)$ has units of volts, then $S_x(f)$ has units of $(\text{W-}\Omega)/\text{Hz}$, and if $x(t)$ has units of amperes, then $S_x(f)$ has units of $(\text{W}/\Omega)/\text{Hz}$. Applying the identity

$$\left|A+B\right|^2 = \left|A\right|^2 + 2\,\text{Re}\left\{AB^*\right\} + \left|B\right|^2 \tag{11.1-43}$$

to (11.1-24) yields

$$\begin{aligned}\left|X(f)\right|^2 &= \frac{1}{4}\left|\tilde{X}(f-f_c)\right|^2 + \frac{1}{4}\left|\tilde{X}^*\left(-[f+f_c]\right)\right|^2 \\ &= \frac{1}{4}\left|\tilde{X}(f-f_c)\right|^2 + \frac{1}{4}\left|\tilde{X}\left(-[f+f_c]\right)\right|^2\end{aligned} \tag{11.1-44}$$

since

$$\tilde{X}(f-f_c)\tilde{X}\left(-[f+f_c]\right) = 0\ , \tag{11.1-45}$$

and by substituting (11.1-44) into (11.1-42), we obtain

$$\boxed{S_x(f) = \frac{1}{4} S_{\tilde{x}}(f - f_c) + \frac{1}{4} S_{\tilde{x}}\big(-[f + f_c]\big)} \tag{11.1-46}$$

where

$$\boxed{S_{\tilde{x}}(f) = \frac{1}{T} \left| \tilde{X}(f) \right|^2} \tag{11.1-47}$$

is the power spectrum of the complex envelope $\tilde{x}(t)$. From (11.1-47) it can be seen that the power spectrum $S_{\tilde{x}}(f)$ of the complex envelope $\tilde{x}(t)$ is also *real* and *nonnegative* ($S_{\tilde{x}}(f) \geq 0$) even though $\tilde{x}(t)$ is *complex* in general.

The time-average power of $x(t)$ can be obtained by integrating its power spectrum $S_x(f)$, that is,

$$P_{\text{avg},x} = \int_{-\infty}^{\infty} S_x(f)\, df . \tag{11.1-48}$$

Since $x(t)$ is *real*, $S_x(f)$ is an *even* function of frequency f because the Fourier transform $X(f)$ satisfies the *conjugate symmetry property* – the magnitude spectrum $|X(f)|$ is an even function of frequency and the phase spectrum $\angle X(f)$ is an odd function of frequency. Therefore, (11.1-48) reduces to

$$\boxed{P_{\text{avg},x} = 2 \int_{0}^{\infty} S_x(f)\, df} \tag{11.1-49}$$

Equation (11.1-49) indicates that we only need to integrate the power spectrum along the positive frequency axis. With the use of (11.1-49), the time-average power of $x(t)$ in the frequency band $\Delta f = f_2 - f_1$ hertz is given by

$$\boxed{P_{\text{avg},x,\Delta f} = 2 \int_{f_1}^{f_2} S_x(f)\, df} \tag{11.1-50}$$

Since the complex envelope $\tilde{x}(t)$ is, in general, a *complex* signal, its power spectrum $S_{\tilde{x}}(f)$ is *not*, in general, an even function of frequency. Therefore, in order to compute the time-average power of $\tilde{x}(t)$, we need to integrate its power spectrum $S_{\tilde{x}}(f)$ along both the negative and positive frequency axes, that is,

$$P_{\text{avg},\tilde{x}} = \int_{-\infty}^{\infty} S_{\tilde{x}}(f)\, df . \tag{11.1-51}$$

Therefore, substituting (11.1-51) into (11.1-41) yields

$$\boxed{P_{\text{avg},x} = \frac{1}{2} P_{\text{avg},\tilde{x}} = \frac{1}{2}\int_{-\infty}^{\infty} S_{\tilde{x}}(f)\,df} \tag{11.1-52}$$

where $P_{\text{avg},x}$ is the time-average power of $x(t)$.

11.1.3 Orthogonality Relationships

In this subsection we shall show that a real bandpass signal $x(t)$ and its Hilbert transform $\hat{x}(t)$ are *orthogonal*, that is, their *inner product* is equal to *zero*. As a result, their Fourier transforms are also orthogonal. The inner product of $x(t)$ and $\hat{x}(t)$ is, by definition,

$$\langle x(t), \hat{x}(t)\rangle \triangleq \int_{-\infty}^{\infty} x(t)\hat{x}^*(t)\,dt\,. \tag{11.1-53}$$

With the use of Parseval's Theorem, (11.1-53) can be rewritten as

$$\langle x(t), \hat{x}(t)\rangle = \langle X(f), \hat{X}(f)\rangle = \int_{-\infty}^{\infty} X(f)\hat{X}^*(f)\,df\,. \tag{11.1-54}$$

Substituting (11.1-10) into (11.1-54) yields

$$\langle x(t), \hat{x}(t)\rangle = \langle X(f), \hat{X}(f)\rangle = j\int_{-\infty}^{\infty} \operatorname{sgn}(f)\left|X(f)\right|^2 df\,, \tag{11.1-55}$$

and since the sign function $\operatorname{sgn}(f)$ is an *odd* function of frequency f and the magnitude spectrum $\left|X(f)\right|$ is an *even* function of f because $x(t)$ is real (a consequence of the conjugate symmetry property for real signals), the integrand in (11.1-55) is an *odd* function of f, and as a result,

$$\boxed{\langle x(t), \hat{x}(t)\rangle = \langle X(f), \hat{X}(f)\rangle = 0} \tag{11.1-56}$$

Therefore, the real bandpass signal $x(t)$ and its Hilbert transform $\hat{x}(t)$ are orthogonal, as well as their Fourier transforms.

11.2 The Complex Envelope of an Amplitude-and-Angle-Modulated Carrier

In this section we shall use the definitions and basic relationships discussed in Section 11.1 and Subsection 11.1.1 to compute the complex envelope, envelope, energy, and time-average power of an amplitude-and-angle-modulated carrier (a real bandpass signal). An amplitude-and-angle-modulated carrier is given by

$$x(t) = a(t)\cos\left[2\pi f_c t + \theta(t)\right], \tag{11.2-1}$$

where $a(t)$ and $\theta(t)$ are real amplitude-modulating and angle-modulating functions, respectively, $\cos(2\pi f_c t)$ is the carrier waveform, and f_c is the carrier frequency in hertz. The amplitude-modulating function $a(t)$ has units of volts or amperes. The angle-modulating function $\theta(t)$ is also known as the *phase deviation* in radians.

The value of the carrier frequency f_c is determined by taking into account the following three main considerations: 1) the bandwidth W in hertz of the complex envelope of the amplitude-and-angle-modulated carrier (see Fig. 11.1-3), 2) the desired 3-dB beamwidth of the far-field beam pattern of the sonar system, and 3) frequency-dependent attenuation due to sound propagation in the ocean. First, in order to avoid signal distortion, $f_c > W$ so that the magnitude spectrum of the bandpass signal along the positive and negative frequency axes do not overlap (see Fig. 11.1-1). Second, when the size of an aperture (array) is fixed, the 3-dB beamwidth of the corresponding far-field beam pattern can be decreased if the operating frequency (carrier frequency f_c) is increased. Third, as the operating frequency increases, attenuation due to sound propagation in the ocean also increases. Therefore, after ensuring $f_c > W$ to avoid signal distortion, there is then a tradeoff between desired beamwidth and short-range versus long-range applications.

Before we begin the derivation of the complex envelope of (11.2-1), let us briefly review some of the basic terminology and equations associated with angle modulation. The *instantaneous phase* (in radians) of $x(t)$ is defined as the argument of the cosine function:

$$\boxed{\theta_i(t) \triangleq 2\pi f_c t + \theta(t)} \tag{11.2-2}$$

The *instantaneous radian frequency* (in radians per second) of $x(t)$ is defined as the time derivative of the instantaneous phase:

$$\boxed{\omega_i(t) \triangleq \frac{d}{dt}\theta_i(t) = 2\pi f_c + \frac{d}{dt}\theta(t)} \tag{11.2-3}$$

Therefore, the *instantaneous frequency* (in hertz) of $x(t)$ is defined as

$$\boxed{f_i(t) \triangleq \frac{1}{2\pi}\frac{d}{dt}\theta_i(t) = f_c + \frac{1}{2\pi}\frac{d}{dt}\theta(t)} \tag{11.2-4}$$

The time derivative $d\theta(t)/dt$ is known as the *frequency deviation* in radians per second.

There are two basic types of angle modulation – *phase modulation* (PM) and *frequency modulation* (FM). Phase modulation implies that the phase deviation $\theta(t)$ of the carrier is directly proportional to some *message* or *modulating signal* $m(t)$, that is,

$$\theta(t) = D_p\, m(t)\,, \tag{11.2-5}$$

where D_p is the *phase-deviation constant* in radians per unit of $m(t)$. Frequency modulation implies that the frequency deviation $d\theta(t)/dt$ of the carrier is directly proportional to $m(t)$, that is,

$$\frac{d}{dt}\theta(t) = D_f\, m(t)\,, \tag{11.2-6}$$

where D_f is the *frequency-deviation constant* in radians per second, per unit of $m(t)$. As a result, the phase deviation of a frequency-modulated carrier is given by

$$\theta(t) = \theta(t_0) + D_f \int_{t_0}^{t} m(\zeta)\, d\zeta\,, \tag{11.2-7}$$

where $\theta(t_0)$ is the phase deviation at $t = t_0$.

We begin the derivation of the complex envelope of (11.2-1) by using the trigonometric identity

$$\cos(\alpha + \beta) = \cos\alpha\cos\beta - \sin\alpha\sin\beta \tag{11.2-8}$$

to rewrite (11.2-1) as follows:

$$\boxed{x(t) = x_c(t)\cos(2\pi f_c t) - x_s(t)\sin(2\pi f_c t)} \tag{11.2-9}$$

where

$$\boxed{x_c(t) = a(t)\cos\theta(t)} \tag{11.2-10}$$

and

$$\boxed{x_s(t) = a(t)\sin\theta(t)} \tag{11.2-11}$$

are known as the *cosine* and *sine components* of $x(t)$, respectively. The functions $x_c(t)$ and $x_s(t)$ are also known as the *in-phase* and *quadrature-phase components*, respectively, because $x_c(t)$ is in-phase with the carrier waveform $\cos(2\pi f_c t)$, and $x_s(t)$ is $90°$ out-of-phase with the carrier waveform.

The next step is to compute the Hilbert transform of $x(t)$. First rewrite (11.2-9) as follows:

$$x(t) = x_c(t)\,x_{\mathrm{BP1}}(t) - x_s(t)\,x_{\mathrm{BP2}}(t)\,, \tag{11.2-12}$$

where

$$x_{\mathrm{BP1}}(t) = \cos(2\pi f_c t) \tag{11.2-13}$$

and

$$x_{\mathrm{BP2}}(t) = \sin(2\pi f_c t) \tag{11.2-14}$$

are real bandpass functions with complex frequency spectra

$$X_{\mathrm{BP1}}(f) = \frac{1}{2}\delta(f - f_c) + \frac{1}{2}\delta(f + f_c) \tag{11.2-15}$$

and

$$X_{\mathrm{BP2}}(f) = \frac{1}{2}\exp\left(-j\pi/2\right)\delta(f - f_c) + \frac{1}{2}\exp\left(+j\pi/2\right)\delta(f + f_c)\,. \tag{11.2-16}$$

Note that the bandpass spectra given by (11.2-15) and (11.2-16) are both centered at $f = \pm f_c$ hertz. Therefore, if both $x_c(t)$ and $x_s(t)$ are *lowpass* functions with bandwidth W hertz, that is, if

$$\left|X_c(f)\right| = 0, \qquad \left|f\right| \geq W\,, \tag{11.2-17}$$

and

$$\left|X_s(f)\right| = 0, \qquad \left|f\right| \geq W\,, \tag{11.2-18}$$

then the Hilbert transform of (11.2-12) is given by

$$\hat{x}(t) = x_c(t)\,\hat{x}_{\mathrm{BP1}}(t) - x_s(t)\,\hat{x}_{\mathrm{BP2}}(t) \tag{11.2-19}$$

provided that

$$\boxed{f_c > W} \tag{11.2-20}$$

Equation (11.2-20) guarantees that $\left|X_c(f)\right|$ and $\left|X_{\mathrm{BP1}}(f)\right|$ do not overlap, and that $\left|X_s(f)\right|$ and $\left|X_{\mathrm{BP2}}(f)\right|$ do not overlap. The following property of the Hilbert transform was used to obtain (11.2-19): if

$$x(t) = x_{\text{LP}}(t)\,x_{\text{BP}}(t)\,, \tag{11.2-21}$$

where $x_{\text{LP}}(t)$ is a lowpass function and $x_{\text{BP}}(t)$ is a bandpass function with non-overlapping magnitude spectra, then

$$\boxed{\hat{x}(t) = x_{\text{LP}}(t)\,\hat{x}_{\text{BP}}(t)} \tag{11.2-22}$$

that is, only the bandpass function is Hilbert transformed. Since the Hilbert transforms of (11.2-13) and (11.2-14) are given by [see (11.1-13) and (11.1-14)]

$$\hat{x}_{\text{BP1}}(t) = \sin(2\pi f_c t) \tag{11.2-23}$$

and

$$\hat{x}_{\text{BP2}}(t) = -\cos(2\pi f_c t)\,, \tag{11.2-24}$$

substituting (11.2-23) and (11.2-24) into (11.2-19) yields the Hilbert transform

$$\boxed{\hat{x}(t) = x_c(t)\sin(2\pi f_c t) + x_s(t)\cos(2\pi f_c t)} \tag{11.2-25}$$

The final two steps are to compute the pre-envelope and complex envelope of $x(t)$. Substituting (11.2-9) and (11.2-25) into (11.1-3) yields the pre-envelope

$$x_p(t) = \left[x_c(t) + j x_s(t)\right]\exp(+j2\pi f_c t)\,, \tag{11.2-26}$$

and by substituting (11.2-26) into (11.1-2), we finally obtain the complex envelope

$$\boxed{\tilde{x}(t) = x_c(t) + j x_s(t)} \tag{11.2-27}$$

where the real, lowpass, cosine and sine components, $x_c(t)$ and $x_s(t)$, with bandwidths W hertz, are given by (11.2-10) and (11.2-11), respectively. Equation (11.2-27) is the complex envelope of the amplitude-and-angle-modulated carrier given by (11.2-1) and is, in general, a complex-valued function of time. Equation (11.2-27) expresses the complex envelope in rectangular form, that is, in terms of real and imaginary parts. The complex envelope can also be expressed in polar form as follows:

$$\tilde{x}(t) = \left|\tilde{x}(t)\right|\exp\left[+j\angle\tilde{x}(t)\right], \tag{11.2-28}$$

where

$$\begin{aligned} |\tilde{x}(t)| &= \sqrt{x_c^2(t) + x_s^2(t)} \\ &= \sqrt{a^2(t)\left[\cos^2\theta(t) + \sin^2\theta(t)\right]} \\ &= a(t) \end{aligned} \tag{11.2-29}$$

and

$$\begin{aligned} \angle\tilde{x}(t) &= \tan^{-1}\left[\frac{x_s(t)}{x_c(t)}\right] = \tan^{-1}\left[\frac{a(t)\sin\theta(t)}{a(t)\cos\theta(t)}\right] \\ &= \tan^{-1}[\tan\theta(t)] \\ &= \theta(t). \end{aligned} \tag{11.2-30}$$

Therefore, substituting (11.2-29) and (11.2-30) into (11.2-28) yields

$$\boxed{\tilde{x}(t) = a(t)\exp[+j\theta(t)]} \tag{11.2-31}$$

where $a(t)$ and $\theta(t)$ are real amplitude-modulating and angle-modulating functions. The polar form of the complex envelope given by (11.2-31) provides a simple way to represent the real amplitude-and-angle-modulated carrier given by (11.2-1). The polar form is the preferred form for doing analysis. Note that if (11.2-31) is substituted into (11.1-6), then we obtain (11.2-1).

If there is no angle modulation, that is, if $\theta(t) = 0$, then $x(t) = a(t)\cos(2\pi f_c t)$,

$$x_c(t) = a(t), \tag{11.2-32}$$

$$x_s(t) = 0, \tag{11.2-33}$$

and

$$\tilde{x}(t) = a(t). \tag{11.2-34}$$

Therefore, the complex envelope is equal to the real amplitude-modulating function when there is no angle modulation.

The envelope of $x(t)$ can be obtained by taking the absolute value of (11.2-29) [see (11.1-7)]. Doing so yields

$$\boxed{\mathcal{E}(t) = |a(t)| \geq 0} \tag{11.2-35}$$

In communication theory, the envelope of a real amplitude-and-angle-modulated carrier is defined by (11.2-35) irrespective of complex envelopes. As was mentioned in Subsection 11.1.1, in real-world problems, $x(t)$ will have a finite duration. If $x(t)$ is defined for $0 \leq t \leq T$, where T is the duration or pulse length of $x(t)$ in seconds, then substituting (11.2-29) into (11.1-38) yields the energy of the complex envelope

$$\boxed{E_{\tilde{x}} = \int_0^T a^2(t)\,dt} \tag{11.2-36}$$

The energy and time-average power of an amplitude-and-angle-modulated carrier are given by [see (11.1-36) and (11.1-41)]

$$\boxed{E_x = \frac{1}{2}E_{\tilde{x}} = \frac{1}{2}\int_0^T a^2(t)\,dt} \tag{11.2-37}$$

and

$$\boxed{P_{\text{avg},\,x} = \frac{E_x}{T} = \frac{1}{2T}\int_0^T a^2(t)\,dt} \tag{11.2-38}$$

As can be seen from (11.2-37) and (11.2-38), the angle-modulating function $\theta(t)$ does *not* contribute to signal energy and, as a result, to time-average power.

11.2.1 The Bandpass Sampling Theorem

Since the complex envelope $\tilde{x}(t)$ is a lowpass (baseband) signal bandlimited to W hertz (see Fig. 11.1-3), the sampling theorem states that $\tilde{x}(t)$ can be reconstructed from its sampled values $\tilde{x}(nT_S)$ as follows:

$$\tilde{x}(t) = \sum_{n=-\infty}^{\infty} \tilde{x}(nT_S)\,\text{sinc}\left(\frac{t - nT_S}{T_S}\right), \tag{11.2-39}$$

where

$$f_S = \frac{1}{T_S} \geq 2W \tag{11.2-40}$$

is the sampling frequency in hertz (a.k.a. the sampling rate in samples per second), T_S is the sampling period in seconds, and

$$\text{sinc}(\alpha) \triangleq \frac{\sin(\pi\alpha)}{\pi\alpha}. \tag{11.2-41}$$

The *minimum* sampling rate is called the *Nyquist rate* and is equal to $2W$ samples per second.

Let $x(t)$ and, hence, $\tilde{x}(t)$ be defined for $0 \le t \le T$, where T is the duration or pulse length of $x(t)$ in seconds. With the use of (11.2-27), (11.2-39) can be rewritten as

$$\tilde{x}(t) = \sum_{n=0}^{N-1} \left[x_c(nT_S) + j x_s(nT_S) \right] \operatorname{sinc}\left(\frac{t - nT_S}{T_S} \right), \tag{11.2-42}$$

where

$$T = (N-1)T_S \tag{11.2-43}$$

and $N = f_S T + 1$ is the number of samples taken of both $x_c(t)$ and $x_s(t)$ for a total of $2N$ samples. Substituting (11.2-42) into (11.1-6) yields

$$x(t) = \sum_{n=0}^{N-1} \operatorname{Re}\left\{ \left[x_c(nT_S) + j x_s(nT_S) \right] \exp(+j2\pi f_c t) \right\} \operatorname{sinc}\left(\frac{t - nT_S}{T_S} \right), \tag{11.2-44}$$

and by expanding the complex exponential using Euler's identity and taking the real part, we obtain

$$\boxed{x(t) = \sum_{n=0}^{N-1} \left[x_c(nT_S)\cos(2\pi f_c t) - x_s(nT_S)\sin(2\pi f_c t) \right] \operatorname{sinc}\left(\frac{t - nT_S}{T_S} \right)} \tag{11.2-45}$$

Equation (11.2-45) is referred to as the *bandpass sampling theorem*. It states that an amplitude-and-angle-modulated carrier $x(t)$ (a real bandpass signal) can be reconstructed from sampled values of its lowpass (baseband) cosine and sine components, $x_c(t)$ and $x_s(t)$.

11.2.2 Orthogonality Relationships

In this subsection we shall show that the cosine and sine components, $x_c(t)$ and $x_s(t)$, of an amplitude-and-angle-modulated carrier $x(t)$ are *orthogonal*, that is, their *inner product* is equal to *zero*. As a result, their Fourier transforms are also orthogonal.

With the use of Parseval's Theorem and (11.2-27), the energy of the complex envelope given by (11.1-29) can also be expressed as

$$E_{\tilde{x}} \triangleq \int_{-\infty}^{\infty} \left| \tilde{x}(t) \right|^2 dt = \int_{-\infty}^{\infty} \left| \tilde{X}(f) \right|^2 df \tag{11.2-46}$$

or

$$E_{\tilde{x}} = \int_{-\infty}^{\infty} x_c^2(t)\,dt + \int_{-\infty}^{\infty} x_s^2(t)\,dt = \int_{-\infty}^{\infty} \left|X_c(f)\right|^2 df + \int_{-\infty}^{\infty} \left|X_s(f)\right|^2 df . \tag{11.2-47}$$

Equating the right-hand sides of (11.2-46) and (11.2-47) yields

$$\int_{-\infty}^{\infty} \left|\tilde{X}(f)\right|^2 df = \int_{-\infty}^{\infty} \left|X_c(f)\right|^2 df + \int_{-\infty}^{\infty} \left|X_s(f)\right|^2 df . \tag{11.2-48}$$

Since [see (11.2-27)]

$$\tilde{X}(f) = X_c(f) + jX_s(f) \tag{11.2-49}$$

and

$$\left|\tilde{X}(f)\right|^2 = \tilde{X}(f)\tilde{X}^*(f) , \tag{11.2-50}$$

substituting (11.2-49) into (11.2-50) yields

$$\left|\tilde{X}(f)\right|^2 = \left|X_c(f)\right|^2 + jX_c^*(f)X_s(f) - jX_c(f)X_s^*(f) + \left|X_s(f)\right|^2 . \tag{11.2-51}$$

Therefore,

$$\begin{aligned}\int_{-\infty}^{\infty} \left|\tilde{X}(f)\right|^2 df = \int_{-\infty}^{\infty} \left|X_c(f)\right|^2 df + \int_{-\infty}^{\infty} \left|X_s(f)\right|^2 df + \\ \left[-j\int_{-\infty}^{\infty} X_c(f)X_s^*(f)\,df\right] + \left[j\int_{-\infty}^{\infty} X_c^*(f)X_s(f)\,df\right]\end{aligned} \tag{11.2-52}$$

or [see (11.1-22)]

$$\begin{aligned}\int_{-\infty}^{\infty} \left|\tilde{X}(f)\right|^2 df = \int_{-\infty}^{\infty} \left|X_c(f)\right|^2 df + \int_{-\infty}^{\infty} \left|X_s(f)\right|^2 df - \\ 2\,\mathrm{Re}\left\{j\int_{-\infty}^{\infty} X_c(f)X_s^*(f)\,df\right\}.\end{aligned} \tag{11.2-53}$$

In order for the right-hand sides of (11.2-48) and (11.2-53) to be equal,

$$\int_{-\infty}^{\infty} X_c(f)X_s^*(f)\,df = \int_{-\infty}^{\infty} x_c(t)x_s^*(t)\,dt = 0 \tag{11.2-54}$$

or

$$\boxed{\left\langle x_c(t), x_s(t)\right\rangle = \left\langle X_c(f), X_s(f)\right\rangle = 0} \tag{11.2-55}$$

Equation (11.2-55) indicates that the cosine and sine components and their Fourier transforms are orthogonal. In other words, their inner products are equal to zero.

11.3 The Quadrature Demodulator

The complex envelope given by (11.2-27) was obtained by evaluating the mathematical definition given by (11.1-2). However, in practical signal-processing applications, the complex envelope given by (11.2-27) can be obtained by passing a real amplitude-and-angle-modulated carrier through a *quadrature demodulator* (QD), if there are *no* frequency and phase offsets. The cosine and sine components can then be used to perform amplitude and angle demodulation. Furthermore, there is no need to compute a Hilbert transform and pre-envelope as we shall show next.

Let the amplitude-and-angle-modulated carrier

$$\begin{aligned} x(t) &= a(t)\cos\left[2\pi f_c t + \theta(t) + \varepsilon\right] \\ &= x_c(t)\cos(2\pi f_c t + \varepsilon) - x_s(t)\sin(2\pi f_c t + \varepsilon) \end{aligned} \tag{11.3-1}$$

be the input signal to the QD shown in Fig. 11.3-1, where $x_c(t)$ and $x_s(t)$ are the cosine and sine components of $x(t)$ given by (11.2-10) and (11.2-11), respectively, and ε is a phase term in radians. We begin by analyzing the *worst* case, that is, when there are both frequency and phase offsets. If there are *frequency offsets*, $f_1 \neq f_c$ and $f_2 \neq f_c$; and *phase offsets*, $\varepsilon_1 \neq \varepsilon$ and $\varepsilon_2 \neq \varepsilon$; then it can be shown that the input signal $x_1(t)$ to the ideal, lowpass filter (ILPF) in the upper channel of the QD is given by

$$x_1(t) = x_{1c}(t) + x_{1s}(t)\,, \tag{11.3-2}$$

where

$$\begin{aligned} x_{1c}(t) = {} & x_c(t)\cos\left[2\pi(f_1 - f_c)t\right]\cos(\varepsilon_1 - \varepsilon) - x_c(t)\sin\left[2\pi(f_1 - f_c)t\right]\sin(\varepsilon_1 - \varepsilon) + \\ & x_c(t)\cos\left[2\pi(f_1 + f_c)t\right]\cos(\varepsilon_1 + \varepsilon) - x_c(t)\sin\left[2\pi(f_1 + f_c)t\right]\sin(\varepsilon_1 + \varepsilon) \end{aligned} \tag{11.3-3}$$

and

$$\begin{aligned} x_{1s}(t) = {} & x_s(t)\cos\left[2\pi(f_1 - f_c)t\right]\sin(\varepsilon_1 - \varepsilon) + x_s(t)\sin\left[2\pi(f_1 - f_c)t\right]\cos(\varepsilon_1 - \varepsilon) - \\ & x_s(t)\cos\left[2\pi(f_1 + f_c)t\right]\sin(\varepsilon_1 + \varepsilon) - x_s(t)\sin\left[2\pi(f_1 + f_c)t\right]\cos(\varepsilon_1 + \varepsilon)\,, \end{aligned} \tag{11.3-4}$$

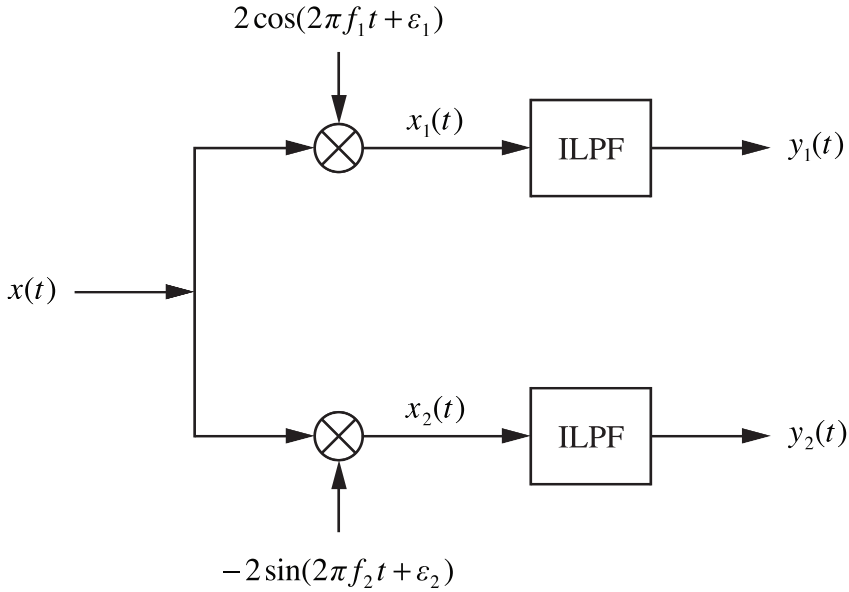

Figure 11.3-1 A quadrature demodulator. The upper channel is referred to as the *I* (in-phase) channel and the lower channel is referred to as the *Q* (quadrature-phase) channel. The acronym ILPF stands for ideal, lowpass filter.

and the input signal $x_2(t)$ to the ILPF in the lower channel of the QD is given by

$$x_2(t) = x_{2c}(t) + x_{2s}(t) \,, \tag{11.3-5}$$

where

$$\begin{aligned} x_{2c}(t) = {} & -x_c(t)\cos\left[2\pi(f_2 - f_c)t\right]\sin(\varepsilon_2 - \varepsilon) - x_c(t)\sin\left[2\pi(f_2 - f_c)t\right]\cos(\varepsilon_2 - \varepsilon) - \\ & x_c(t)\cos\left[2\pi(f_2 + f_c)t\right]\sin(\varepsilon_2 + \varepsilon) - x_c(t)\sin\left[2\pi(f_2 + f_c)t\right]\cos(\varepsilon_2 + \varepsilon) \end{aligned} \tag{11.3-6}$$

and

$$\begin{aligned} x_{2s}(t) = {} & x_s(t)\cos\left[2\pi(f_2 - f_c)t\right]\cos(\varepsilon_2 - \varepsilon) - x_s(t)\sin\left[2\pi(f_2 - f_c)t\right]\sin(\varepsilon_2 - \varepsilon) - \\ & x_s(t)\cos\left[2\pi(f_2 + f_c)t\right]\cos(\varepsilon_2 + \varepsilon) + x_s(t)\sin\left[2\pi(f_2 + f_c)t\right]\sin(\varepsilon_2 + \varepsilon). \end{aligned} \tag{11.3-7}$$

The complex frequency response of an ILPF is given by

$$H(f) = G\exp(-j2\pi f t_0)\operatorname{rect}\left[f/(2B)\right], \tag{11.3-8}$$

where $G > 0$ is the dimensionless gain of the filter, t_0 is the constant time delay of the filter in seconds,

$$\text{rect}\left(\frac{f}{2B}\right) = \begin{cases} 1, & |f| \le B \\ 0, & |f| > B \end{cases} \tag{11.3-9}$$

and B is the bandwidth of the filter in hertz, also referred to as the passband. The magnitude and phase responses of the filter are given by

$$|H(f)| = G\,\text{rect}[f/(2B)] \tag{11.3-10}$$

and

$$\angle H(f) = -2\pi f t_0 \,\text{rect}[f/(2B)], \tag{11.3-11}$$

respectively (see Fig. 11.3-2). The slope of the straight line in the phase response is equal to $-2\pi t_0$.

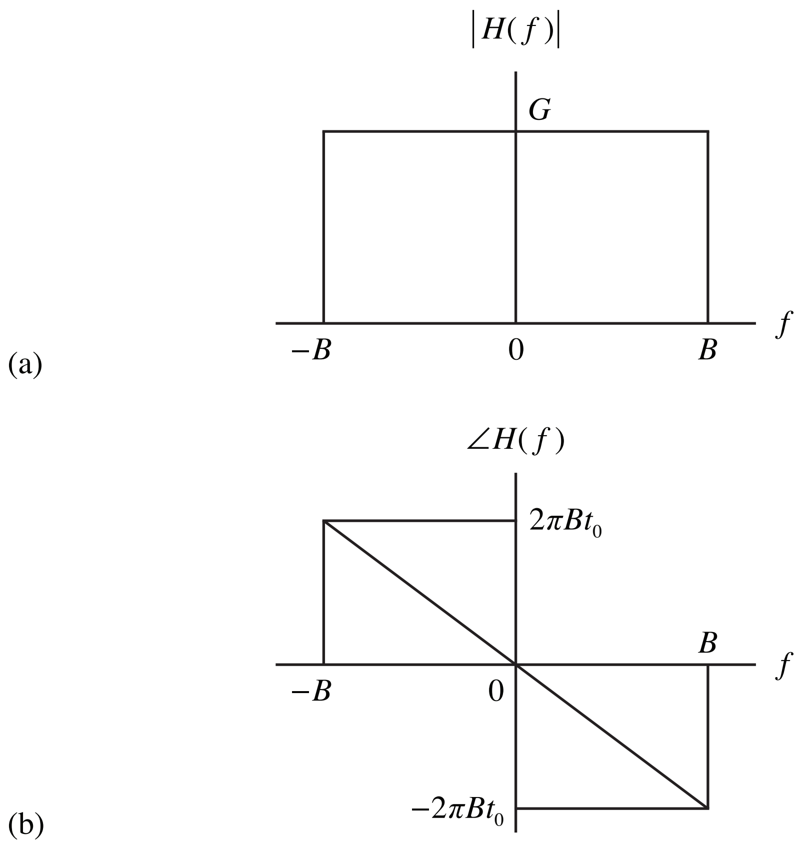

Figure 11.3-2 (a) Magnitude response and (b) phase response of an ideal, lowpass filter.

If $f_1 \approx f_c$ and $f_2 \approx f_c$, then $f_1 - f_c \approx 0$, $f_1 + f_c \approx 2f_c$, $f_2 - f_c \approx 0$, and $f_2 + f_c \approx 2f_c$. Therefore, if the bandwidth (passband) of the ILPFs $B = W$ Hz, which is the bandwidth of the lowpass cosine and sine components [see (11.2-17) and (11.2-18)], and $f_c > W$ [see (11.2-20)], then the output signal $y_1(t)$ from the ILPF in the upper channel (the *I* channel) of the QD is given by

$$y_1(t) = y_{1c}(t) + y_{1s}(t), \tag{11.3-12}$$

where

$$\begin{aligned} y_{1c}(t) \approx Gx_c(t-t_0)\cos\left[2\pi(f_1 - f_c)(t-t_0)\right]\cos(\varepsilon_1 - \varepsilon) - \\ Gx_c(t-t_0)\sin\left[2\pi(f_1 - f_c)(t-t_0)\right]\sin(\varepsilon_1 - \varepsilon) \end{aligned} \tag{11.3-13}$$

and

$$\begin{aligned} y_{1s}(t) \approx Gx_s(t-t_0)\cos\left[2\pi(f_1 - f_c)(t-t_0)\right]\sin(\varepsilon_1 - \varepsilon) + \\ Gx_s(t-t_0)\sin\left[2\pi(f_1 - f_c)(t-t_0)\right]\cos(\varepsilon_1 - \varepsilon), \end{aligned} \tag{11.3-14}$$

and the output signal $y_2(t)$ from the ILPF in the lower channel (the *Q* channel) of the QD is given by

$$y_2(t) = y_{2c}(t) + y_{2s}(t), \tag{11.3-15}$$

where

$$\begin{aligned} y_{2c}(t) \approx -Gx_c(t-t_0)\cos\left[2\pi(f_2 - f_c)(t-t_0)\right]\sin(\varepsilon_2 - \varepsilon) - \\ Gx_c(t-t_0)\sin\left[2\pi(f_2 - f_c)(t-t_0)\right]\cos(\varepsilon_2 - \varepsilon) \end{aligned} \tag{11.3-16}$$

and

$$\begin{aligned} y_{2s}(t) \approx Gx_s(t-t_0)\cos\left[2\pi(f_2 - f_c)(t-t_0)\right]\cos(\varepsilon_2 - \varepsilon) - \\ Gx_s(t-t_0)\sin\left[2\pi(f_2 - f_c)(t-t_0)\right]\sin(\varepsilon_2 - \varepsilon). \end{aligned} \tag{11.3-17}$$

The output signals given by (11.3-13) and (11.3-14), and (11.3-16) and (11.3-17), are shown as being approximate because $f_1 - f_c \neq 0$ and $f_2 - f_c \neq 0$. If $f_1 - f_c \neq 0$ and $f_2 - f_c \neq 0$, then the ILPFs will filter out some of the high frequency components contained in the input signals to the ILPFs involving $f_1 - f_c$ and $f_2 - f_c$ because the magnitude spectra of these input signals are *not* centered at $f = 0$ Hz. These output signals are unacceptable because of the frequency and phase offsets even though $f_1 - f_c \approx 0$ and $f_2 - f_c \approx 0$. Ideally, we want $y_1(t)$ to be equal to an amplitude-scaled and time-delayed version of $x_c(t)$ alone, and $y_2(t)$ to be equal to an amplitude-scaled and time-delayed version of $x_s(t)$ alone.

If there are *no* frequency offsets, that is, if $f_1 = f_c$ and $f_2 = f_c$, then

$$x_{1c}(t) = x_c(t)\cos(\varepsilon_1 - \varepsilon) + x_c(t)\cos\left[2\pi(2f_c)t\right]\cos(\varepsilon_1 + \varepsilon) - x_c(t)\sin\left[2\pi(2f_c)t\right]\sin(\varepsilon_1 + \varepsilon), \tag{11.3-18}$$

$$x_{1s}(t) = x_s(t)\sin(\varepsilon_1 - \varepsilon) - x_s(t)\cos\left[2\pi(2f_c)t\right]\sin(\varepsilon_1 + \varepsilon) - x_s(t)\sin\left[2\pi(2f_c)t\right]\cos(\varepsilon_1 + \varepsilon), \tag{11.3-19}$$

$$x_{2c}(t) = -x_c(t)\sin(\varepsilon_2 - \varepsilon) - x_c(t)\cos\left[2\pi(2f_c)t\right]\sin(\varepsilon_2 + \varepsilon) - x_c(t)\sin\left[2\pi(2f_c)t\right]\cos(\varepsilon_2 + \varepsilon), \tag{11.3-20}$$

and

$$x_{2s}(t) = x_s(t)\cos(\varepsilon_2 - \varepsilon) - x_s(t)\cos\left[2\pi(2f_c)t\right]\cos(\varepsilon_2 + \varepsilon) + x_s(t)\sin\left[2\pi(2f_c)t\right]\sin(\varepsilon_2 + \varepsilon). \tag{11.3-21}$$

Therefore,

$$y_{1c}(t) = Gx_c(t - t_0)\cos(\varepsilon_1 - \varepsilon)\,, \tag{11.3-22}$$

$$y_{1s}(t) = Gx_s(t - t_0)\sin(\varepsilon_1 - \varepsilon)\,, \tag{11.3-23}$$

$$y_{2c}(t) = -Gx_c(t - t_0)\sin(\varepsilon_2 - \varepsilon)\,, \tag{11.3-24}$$

and

$$y_{2s}(t) = Gx_s(t - t_0)\cos(\varepsilon_2 - \varepsilon)\,. \tag{11.3-25}$$

These output signals are still unacceptable because of the phase offsets.

Finally, if in addition to no frequency offsets there are *no* phase offsets, that is, if $\varepsilon_1 = \varepsilon$ and $\varepsilon_2 = \varepsilon$, then

$$x_{1c}(t) = x_c(t) + x_c(t)\cos\left[2\pi(2f_c)t\right]\cos(2\varepsilon) - x_c(t)\sin\left[2\pi(2f_c)t\right]\sin(2\varepsilon)\,, \tag{11.3-26}$$

$$x_{1s}(t) = -x_s(t)\cos\left[2\pi(2f_c)t\right]\sin(2\varepsilon) - x_s(t)\sin\left[2\pi(2f_c)t\right]\cos(2\varepsilon)\,, \tag{11.3-27}$$

$$x_{2c}(t) = -x_c(t)\cos\left[2\pi(2f_c)t\right]\sin(2\varepsilon) - x_c(t)\sin\left[2\pi(2f_c)t\right]\cos(2\varepsilon)\,, \tag{11.3-28}$$

and

$$x_{2s}(t) = x_s(t) - x_s(t)\cos\left[2\pi(2f_c)t\right]\cos(2\varepsilon) + x_s(t)\sin\left[2\pi(2f_c)t\right]\sin(2\varepsilon)\,. \tag{11.3-29}$$

Therefore,

$$\boxed{y_1(t) = Gx_c(t - t_0)} \tag{11.3-30}$$

and

$$\boxed{y_2(t) = Gx_s(t - t_0)} \tag{11.3-31}$$

where $G > 0$ is the dimensionless gain of the ILPFs in the QD, and t_0 is the constant time delay of the ILPFs.

Equations (11.3-30) and (11.3-31) indicate that when there are *no* frequency and phase offsets, the output signals $y_1(t)$ and $y_2(t)$ from the QD shown in Fig. 11.3-1 are amplitude-scaled and time-delayed versions of the cosine and sine components of the amplitude-and-angle-modulated carrier $x(t)$, given by (11.3-1), at the input to the QD. The cosine and sine components are the real and imaginary parts of the complex envelope $\tilde{x}(t)$ of $x(t)$ [see (11.2-27)]. Signal processing algorithms can be used to drive frequency and phase offsets to zero. By properly combining $y_1(t)$ and $y_2(t)$ given by (11.3-30) and (11.3-31), $x(t)$ can be *demodulated*. For example,

$$\boxed{\sqrt{y_1^2(t) + y_2^2(t)} = Ga(t - t_0)} \tag{11.3-32}$$

which is an amplitude-scaled and time-delayed version of the amplitude-modulating function $a(t)$, and

$$\boxed{\tan^{-1}\left[y_2(t)/y_1(t)\right] = \theta(t - t_0)} \tag{11.3-33}$$

which is a time-delayed version of the angle-modulating function $\theta(t)$. Since the values for $\theta(t - t_0)$ obtained from the arctangent function lie in the interval $[-\pi, \pi]$, that is, $-\pi \le \theta(t - t_0) \le \pi$, depending on the kind of angle modulation used, *phase unwrapping* may be necessary in order to obtain the full range of values for $\theta(t - t_0)$.

Problems

Section 11.1

11-1 Use (11.1-8) to verify

(a) (11.1-13)

(b) (11.1-14)

11-2 If the power spectrum $S_{\tilde{x}}(f)$ of the complex envelope $\tilde{x}(t)$ is given as shown in Fig. P11-2, then plot the power spectrum $S_x(f)$ of the real bandpass signal $x(t)$.

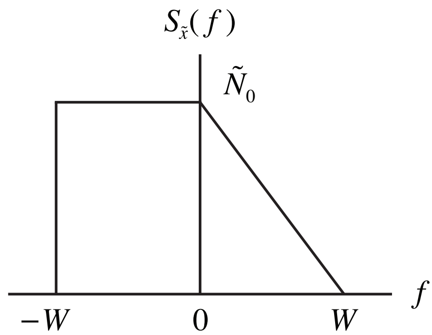

Figure P11-2

Section 11.2

11-3 A very common transmitted electrical signal used in active sonar (and radar) systems is the *rectangular-envelope*, *CW* (continuous-wave) *pulse* given by

$$x(t) = A\cos(2\pi f_c t), \qquad 0 \le t \le T,$$

where the amplitude factor A is a positive constant with units of volts, and T is the pulse length of $x(t)$ in seconds.

(a) Find the complex envelope of $x(t)$.

(b) Find the envelope of $x(t)$.

(c) Find the energy of $x(t)$ with the correct units.

(d) Find the time-average power of $x(t)$ with the correct units.

11-4 Another very common transmitted electrical signal used in active sonar (and radar) systems is the *rectangular-envelope*, *LFM* (linear-frequency-modulated) *pulse* given by

$$x(t) = A\cos\left[2\pi f_c t + \theta(t)\right], \qquad 0 \le t \le T,$$